Molecular Mechanisms of Disease for Mutations at Gly-90 in Rhodopsin*

Darwin Toledo[‡1], **Eva Ramon**[‡1], **Mònica Aguilà**[‡], **Arnau Cordomí**[§], **Juan J. Pérez**[¶], **Hugo F. Mendes**[∥], **Michael E. Cheetham**[∥], and **Pere Garriga**[‡2]

From the [‡]*Centre de Biotecnologia Molecular, Departament d'Enginyeria Química, Universitat Politècnica de Catalunya, 08222 Terrassa, Spain, the [§]Laboratori de Medicina Computacional, Unitat de Bioestadística, Facultat de Medicina, Universitat Autònoma de Barcelona, 08193 Cerdanyola del Vallès, Spain, the [¶]Centre de Biotecnologia Molecular, Departament d'Enginyeria Química, Universitat Politècnica de Catalunya, 08034 Barcelona, Spain, and the [∥]University College London Institute of Ophthalmology, 11-43 Bath Street, London EC1V 9EL, United Kingdom*

Background: Mutations at Gly-90 in rhodopsin cause two different phenotypes: retinitis pigmentosa and congenital night blindness.
Results: G90V retinitis pigmentosa mutant shows constitutive activity and very low thermal stability in the dark state.
Conclusion: Low conformational stability can trigger retinitis pigmentosa associated with rhodopsin mutations.
Significance: Retinoids can help to stabilize the conformation of retinitis pigmentosa mutants.

Two different mutations at Gly-90 in the second transmembrane helix of the photoreceptor protein rhodopsin have been proposed to lead to different phenotypes. G90D has been classically associated with congenital night blindness, whereas the newly reported G90V substitution was linked to a retinitis pigmentosa phenotype. Here, we used Val/Asp replacements of the native Gly at position 90 to unravel the structure/function divergences caused by these mutations and the potential molecular mechanisms of inherited retinal disease. The G90V and G90D mutants have a similar conformation around the Schiff base linkage region in the dark state and same regeneration kinetics with 11-*cis*-retinal, but G90V has dramatically reduced thermal stability when compared with the G90D mutant rhodopsin. The G90V mutant also shows, like G90D, an altered photobleaching pattern and capacity to activate Gt in the opsin state. Furthermore, the regeneration of the G90V mutant with 9-*cis*-retinal was improved, achieving the same A_{280}/A_{500} as wild type isorhodopsin. Hydroxylamine resistance was also recovered, indicating a compact structure around the Schiff base linkage, and the thermal stability was substantially improved when compared with the 11-*cis*-regenerated mutant. These results support the role of thermal instability and/or abnormal photoproduct formation in eliciting a retinitis pigmentosa phenotype. The improved stability and more compact structure of the G90V mutant when it was regenerated with 9-*cis*-retinal brings about the possibility that this isomer or other modified retinoid analogues might be used in potential treatment strategies for mutants showing the same structural features.

Vertebrate rhodopsin is a membrane protein of the family A of G-protein-coupled receptors. Rhodopsin functions as the dim light photoreceptor to the rod cell of the vertebrate retina. In its basal state, rhodopsin consists of a polypeptide chain, opsin, covalently bound through a Schiff base (SB)[3] linkage to its cognate chromophore, the vitamin A aldehyde derivative 11-*cis*-retinal, which acts as an inverse agonist preventing G-protein activation in the dark (1, 2). Rhodopsin mutations have been correlated with congenital retinopathies like retinitis pigmentosa (RP) and congenital stationary night blindness (CSNB) (3). RP is a clinically and genetically heterogeneous trait characterized by impaired night and day vision due to photoreceptor cell degeneration that can eventually lead to total blindness. RP mutations can be found in all three domains of rhodopsin (intradiscal, cytoplasmic, and transmembrane domains). Although protein misfolding or altered trafficking are considered to be the major biochemical consequence of many RP mutations (4–7), some of them have been described as not inducing major structural defects (8, 9), widening the range of potential molecular mechanisms behind rhodopsin RP mutations.

Unlike progressive RP, night blindness is a clinical symptom of various, mostly stationary retinal diseases, characterized by poor dim light adaptation and less severe rod cell degeneration, if any. To date, only four rhodopsin mutations have been associated with CSNB, all of them affecting amino acid residues near the protonated SB linkage between the opsin polypeptide and its chromophore 11-*cis*-retinal (10–13). CSNB mutants induce changes in the receptor conformational stability and the protonation state of the SB nitrogen, altering the UV-visible behavior of the mutant pigments. *In vitro* and *in vivo* studies

[3] The abbreviations used are: SB, Schiff base; adRP, autosomal dominant retinitis pigmentosa; CSNB, congenital stationary night blindness; DM, *n*-dodecyl-*β*-D-maltoside; MetaII, metarhodopsin II; PM, plasma membrane; TM, transmembrane; RP, retinitis pigmentosa; ER, endoplasmic reticulum; GTP*γ*S, guanosine 5′-3-*O*-(thio)triphosphate.

have showed that all CSNB mutations lead to constitutively active receptors (14).

At position Gly-90, in rhodopsin second transmembrane (TM) helix, two different naturally occurring mutations have been reported, each leading to distinct phenotypes. The G90D mutation has been described as causing CSNB, and it has been extensively characterized. G90D rhodopsin activates the visual cascade in the dark or without chromophore (15); *in vivo* this feature can lead to receptor desensitization and signal decrease in response to the light stimulation of the visual cascade. The mutant G90V was reported in a Swiss family with clinical features of the RP phenotype (16). This is the first time that different amino acid substitutions of the same residue have led to distinct phenotypes in rhodopsin.

Considerable efforts have been taken to establish, in a comprehensive manner, the molecular mechanisms underlying congenital retinal disease associated with mutations in the rod opsin gene. In an attempt to address this issue in the present work, we perform a cellular, biochemical, and spectroscopic comparative study of Asp and Val substitutions at position 90 of rhodopsin to assess differences in the genotype-phenotype correlation associated to these mutants. We also analyzed the influence on the receptor stability and UV-visible spectroscopic behavior of 9-*cis*-retinal in the G90V mutant rhodopsin.

We find that the G90V and G90D mutants are very similar in many respects, including their spectroscopic features and cellular processing with primary localization to the plasma membrane (PM), indicating no misfolding of the receptor in the endoplasmic reticulum (ER). Hydroxylamine reactivity, photobleaching behavior, and their ability to activate the G-protein transducin are also comparable. The main difference observed between the two mutants is the low thermal stability in the dark for the autosomal dominant RP (adRP) G90V mutant as compared with the CSNB G90D. Furthermore, regeneration of the G90V mutant with 9-*cis*-retinal improves its dark thermal stability and is in agreement with the proposed role of retinoids as stabilizing molecules that can ameliorate the RP phenotype in certain cases.

EXPERIMENTAL PROCEDURES

Materials—11-*cis*-Retinal was kindly provided by A. R. de Lera (Universidad de Vigo, Spain) and Rosalie Crouch (University of South Carolina and NEI, National Institutes of Health). Purified mAb rho-1D4 was obtained from the National Culture Center (Minneapolis, MN) and was coupled to CNBr-activated Sepharose 4B Fast Flow (Amersham Biosciences). *n*-Dodecyl-β-D-maltoside (DM) was purchased from Anatrace (Maumee, OH). Complete$^{\text{TM}}$ protease inhibitor mixture was from Roche Applied Science and was used at a concentration of 1 tablet/75 ml of buffer. 9-*cis*-retinal was from Sigma-Aldrich.

Cellular Materials—COS-1 cells (ATCC number CRL-1650) were from the American Type Culture Collection (Manassas, VA). SK-N-SH human Caucasian neuroblastoma cells were obtained from the European Collection of Cell Cultures (ECACC, Salisbury, UK). Tissue culture medium, antibiotics, and Lipofectamine were from Invitrogen. 4′,6-Diamidino-2-phenylindole dihydrochloride (DAPI) was from Sigma-Aldrich.

Buffers—The solutions used are defined as follows: Buffer A (137 mM NaCl, 2.7 mM KCl, 1.5 mM KH$_2$PO$_4$, and 8 mM Na$_2$HPO$_4$, pH 7.2); Buffer C (0.05% DM in buffer A, pH 7.2); Buffer D (0.05% DM in 2 mM Na$_2$P$_i$, pH 6.0).

Construction, Expression, and Purification of the Mutant Receptors—Opsin mutants were constructed with a site-directed mutagenesis kit (QuikChange, Stratagene) on a synthetic bovine opsin gene (17) or green fluorescent protein (GFP)-tagged rod opsin using wild type (WT) opsin-GFP (WT-GFP) as a template (18). The expression and purification of the visual receptors were performed as follows. Plasmids encoding the WT or mutant rhodopsin genes were transfected into five COS-1 cells plates at 85% confluence, by using DEAE-dextran with 15 μg of plasmid DNA/145-cm plate. Cells were harvested 48–60 h after transfection, and pigments were reconstituted with 10 μM 11-*cis*-retinal (or 9-*cis*-retinal) in intact cells and then solubilized with 1% (w/v) DM in Buffer A. The pigments were purified by immunoaffinity chromatography on 1D4-Sepharose 4B in Buffer C or Buffer D. All procedures, up to and including binding of the receptor to the immunoaffinity matrix, were performed at 4 °C, whereas subsequent washes and elutions were performed at room temperature using cold buffer. The resin was washed three times with Buffer C, followed by three times with Buffer D. The receptors were eluted in either Buffer C or D containing 100 μM rho-1D4 9-mer peptide (TETSQVAPA). Elution in Buffer C was used for determining the A_{280}/A_{500} ratio corresponding to the overall eluted protein (including the correctly folded and misfolded fractions). However, the different characterization experiments performed were carried out with proteins eluted in Buffer D that correspond to the correctly folded protein fractions (19), and this fact is clearly stated in each experiment.

WT and Mutant Opsin and Rhodopsin Membrane Preparation—Cells were collected 48 h after transfection by using 5 ml of Buffer A/plate and were centrifuged for 5 min at 2400 rpm. The supernatant was discarded, and the pellet was resuspended in 15 mM Tris-HCl, pH 7.5, containing 2 mM MgCl$_2$, 1 mM DTT, and 100 μM PMSF (2 ml/plate) and incubated on ice for 40 min. Then cells were homogenized and spun down for 1 min at 800 rpm at 4 °C in order to remove cell debris and non-homogenized material. The supernatant was then centrifuged for 30 min at 35,000 rpm, 4 °C; the pellet was resuspended with Buffer A; and the sample was split into two tubes. One tube was kept for opsin experiments, and the other was regenerated with 11-*cis*-retinal to be used as rhodopsin samples.

Cellular Expression—Cellular analysis of rod opsin localization was performed essentially as described previously (20). Briefly, SK-N-SH cells were transfected with rod opsin-GFP plasmids using Lipofectamine enhanced with Plus reagent according to the manufacturer's instructions. 24 h after transfection, cells were washed three times with cold PBS, followed by fixation with 3.7% paraformaldehyde. Cells were then washed in PBS, and nuclei were counterstained with 2 μg/ml DAPI before mounting. Transfected cells were assessed for the rod opsin-GFP subcellular localization and scored for the predominant localization, PM, ER, or cells with inclusions, as a percentage of all transfected cells. A cell would be scored as

"PM" if there was PM staining with intracellular staining at a level that could reflect normal opsin biogenesis (*i.e.* some ER and Golgi staining). A cell with intracellular retention of rod opsin and little or no PM staining would be scored as "ER." Cells with any intracellular inclusions (regardless of other cellular staining) would be scored as "inclusions." The scoring was done blind to mutation status. For each construct, $4 \times \sim100$ cells were counted, and each experiment was repeated at least three times. Fluorescence was visualized using a Zeiss LSM 510 laser-scanning confocal microscope, and images were processed and annotated using Adobe Photoshop and Illustrator.

UV-visible Absorption Spectra of WT and Rhodopsin Mutants—All measurements were made on a Cary 100Bio spectrophotometer (Varian), equipped with water-jacketed cuvette holders connected to a circulating water bath. Temperature was controlled by a Peltier accessory connected to the spectrophotometer. All spectra were recorded in the 250–650 nm range with a bandwidth of 2 mm, a response time of 0.1 s, and a scan speed of 300 nm/min. The molar extinction coefficient (ϵ) of each mutant was determined by an acid denaturation method (21). Each ϵ value was calculated from the formula, $\epsilon = (A/A_{Rh})(A_{440Rh}/A_{440})\epsilon_{Rh}$, where A is the absorbance at the λ_{max} value, A_{440} is the absorbance at 440 nm after acid denaturation, and ϵ_{Rh} is the molar extinction of rhodopsin (42.7×10^3 M^{-1} cm^{-1}). The spectral ratio, which was used as a measure of pigment yield and stability, is defined as A_{280} divided by A at the visible λ_{max} value after correction for any difference of the mutant pigment ϵ value as described above.

Photobleaching and Acidification of Purified Rhodopsins—Samples were bleached with a 150-watt power source equipped with an optic fiber guide and using a 495-nm cut-off filter. Dark-adapted pigments were illuminated for 10 s to ensure complete photoconversion to 380-nm absorbing species. Acidification was carried out, immediately after photobleaching, by the addition of $2 N H_2SO_4$ to a final pH of 1.9, and after 2 min, an absorption spectrum was subsequently recorded. Photobleaching of the samples for different time periods was performed for G90D and G90V in Buffer C at different pH values.

Thermal Bleaching Assay—Rhodopsin thermal bleaching rates, in the dark, were obtained by monitoring the decrease of $A_{\lambda max}$ of the visible spectral band and the appearance of A_{380} as a function of time at either 48 or 55 °C. Spectra were recorded every 2.5 min. Data points were obtained by using the equation, $\Delta A = (A - A_f)/(A_0 - A_f)$, where A is the absorbance recorded at λ_{max}, A_f is the absorbance at the final time, and A_0 is the absorbance at time 0, and were fit to a single exponential decay function.

Regeneration of Rhodopsin—Free 11-*cis*-retinal, in an ethanol stock solution, was added to a 2.5-fold molar excess over dark-adapted pigments. Then the sample was illuminated with a yellow cut-off filter (>495 nm) to avoid photobleaching of the free retinal, and successive spectra were registered, at 20 °C in the dark, every 5 min until no further increase in $A_{\lambda max}$ was detected.

Reaction of Mutant Rhodopsin Pigments with Hydroxylamine—A solution of hydroxylamine hydrochloride, adjusted to pH 7 with NaOH, was added to dark-adapted samples in Buffer D (final concentration of 50 mM), and successive spectra were recorded every 5 min to monitor the loss of pigment (A_{max}) and formation of retinal oxime ($A_{365 nm}$). Reactions were carried out in the dark at 20 °C.

Metarhodopsin II (MetaII) Decay Measurements—The MetaII active conformation decay process was followed in real time by fluorescence spectroscopy (22). Briefly, 0.5 μM Rho in Buffer C was kept at 20 °C for 10 min and illuminated for 30 s. The $t_{1/2}$ values of Trp fluorescence increase, due to retinal release, were determined by fitting the experimental data to a single-exponential curve using Sigma Plot version 11.0 (Systat Software, Inc., Chicago, IL). Fluorescence assays were performed using a Photon Technologies QM-1 steady state fluorescence spectrophotometer (PTI Technologies, Birmingham, NJ). Sample temperature was controlled with a cuvette holder Peltier accessory TLC 50 (Quantum Northwest, Liberty Lake, WA) connected to a hybrid liquid coolant system Reserator XT (Zalman, Garden Grove, CA). All fluorescence spectra were carried out by exciting the samples for 2 s at $\lambda = 295$ nm and a bandwidth slit of 0.5 nm, and blocking the excitation beam for 28 s, to avoid further photobleaching of the sample. Trp emission was monitored at $\lambda = 330$ nm and a bandwidth slit of 5 nm. Experiments were done in triplicate.

Transducin Activation Assays for WT and Mutant Rhodopsins and Opsins—Transducin activation was determined in COS-1 cell membranes, and the ability of opsin and rhodopsin to activate transducin was monitored with a radionucleotide filter binding assay by measuring the uptake of [^{35}S]GTPγS by transducin purified from bovine retinas. The assays were performed by mixing 6 nM mutant rhodopsin or opsin in membranes with 500 nM transducin in 25 mM Tris, pH 7.5, 100 mM NaCl, 5 mM magnesium acetate, 5% glycerol, 2.5 mM DTT, and 3 μM [^{35}S]GTPγS (0.128 Ci/mmol) at room temperature. Reactions were initiated by the addition of rhodopsin or opsin in the dark, and samples were filtrated after different incubation times, either in the dark or after illumination, to determine the amount of bound [^{35}S]GTPγS.

RESULTS

Subcellular Localization of Gly-90 Mutants in SK-N-SH Cells—The heterologous expression of rhodopsin in cell culture can be used to monitor protein biogenesis, traffic, and purification for functional studies. SK-N-SH neuroblastoma cells have been used to study the biogenesis, degradation, aggregation, and traffic of WT and mutant forms of rod opsin tagged at their C terminus with GFP (9, 23). WT rod opsin-GFP (WT-GFP) trafficked to the PM with great efficiency (94% of transfected cells), and only occasionally was it predominantly retained in the ER (3% of cells) or formed intracellular inclusions (3% of cells) (Fig. 1*A*). The G90V or G90D amino acid substitutions in rod opsin did not affect traffic in SK-N-SH cells (Fig. 1, *B* and *C*). G90V-GFP and G90D-GFP both trafficked to the PM in the majority of cells (88 and 90%, respectively), and only a few cells showed predominant retention in the ER or inclusion formation. Western blotting revealed that the electrophoretic mobility and expression level of G90D and G90V were identical to that of WT rhodopsin (data not shown). Therefore, the substitution of Gly-90 for Asp or Val does not appear to cause a major defect in rhodopsin biogenesis like class II mutants, such as P23H, which
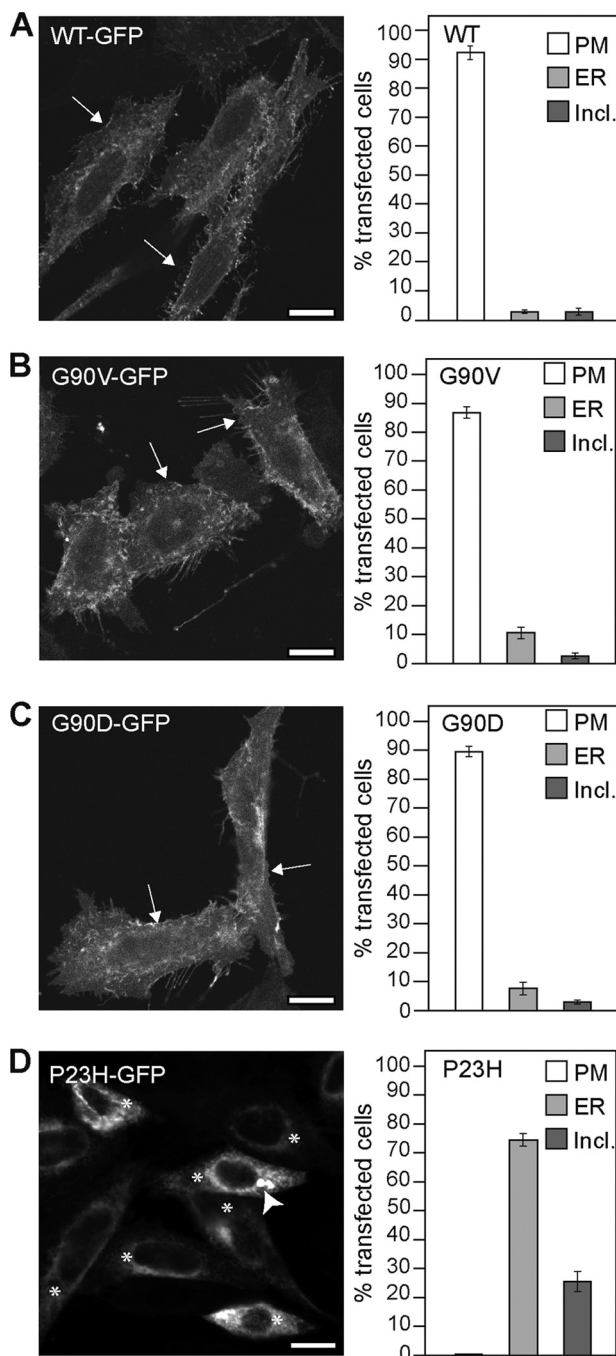
FIGURE 1. **Subcellular localization of WT, G90V, G90D, and P23H mutants in SK-N-SH cells.** SK-N-SH cells were transfected with WT-GFP (*A*), G90V-GFP (*B*), G90D-GFP (*C*), and P23H-GFP (*D*) fixed after 24 h. Representative images of rod opsin-GFP localization are shown in each *panel* with a quantification of the percentage of cells with predominant localization at the PM (*white*), ER (*gray*), or inclusions (*Incl.; dark gray*). Note that WT-GFP, G90V-GFP, and G90D-GFP were predominantly trafficked to the PM (*arrow*). ER retention (*) and inclusions (*arrowhead*) are indicated in the P23H-GFP for better comparison. *Scale bar*, 10 μm. *Error bars*, 2 × ±S.E.

lead to protein misfolding, ER retention (Fig. 1*D*), and failure to traffic through the secretory pathway (9, 23).

UV-visible Spectrophotometry of Immunopurified Gly-90 Rhodopsin Mutants—The UV-visible spectra of WT and G90D and G90V mutant rhodopsins in Buffer C were recorded in the dark, after illumination for 10 s and after subsequent acidification (Fig. 2). A summary of the spectral parameters, including
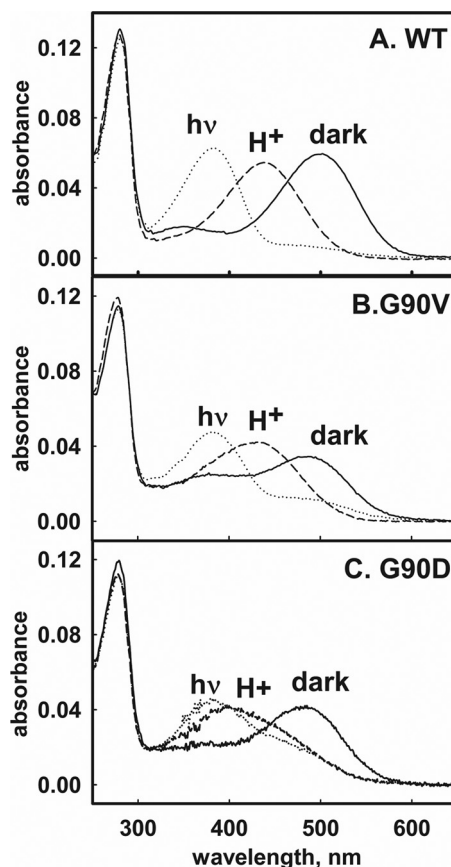

FIGURE 2. **UV-visible characterization of the immunopurified WT and mutant pigments.** UV-visible spectra of WT (*A*) and G90V (*B*) and G90D mutants (*C*) in the basal state (*dark*), upon light stimulation (*hν*), and after acidification (*H+*) are shown. Spectra were recorded in Buffer C at 20 °C. The G90V mutant is able to form pigment readily to about WT levels, with a slightly blue-shifted maximum according to UV-visible spectrophotometric measurements.

λ_{max} value of the visible chromophoric band, molar extinction coefficient (ϵ), and spectral ratio ($A_{280\ nm}$ *versus* absorbance at the visible λ_{max} value), in Buffer C is shown in Table 1. The G90V mutant is able to form pigment readily with a slightly blue-shifted maximum at 489 nm when compared with WT rhodopsin and to a similar extent as the G90D mutant. The slightly increased A_{280}/A_{500} ratio, in the case of G90V, could be reflecting either that the Gly→Val substitution causes a small fraction of misfolded protein or the lack of structural stability of the rhodopsin mutant. The main difference in the dark ground state spectrum of G90V compared with G90D was that the RP mutant showed a higher $A_{380\ nm}$ with regard to the $A_{489\ nm}$ visible band. Precisely, G90V showed a $A_{380\ nm}/A_{489\ nm}$ ratio of 0.67 compared with the G90D ratio of 0.55 and the $A_{380\ nm}/A_{500\ nm}$ for WT of 0.25. Both mutants showed abnormal photobleaching patterns, after 10-s illumination, with a photoproduct species absorbing at ~490 nm detected for the G90V mutant (accounting for about 25% of the dark visible band) as well as for the G90D (50% of the dark visible band; λ_{max} ~475 nm) (Fig. 2, *B* and *C*). Photobleaching was facilitated by increasing either the pH to 8.0 or by longer light exposure times (data not shown). Acidification of these photoactivated receptors resulted in distinctive behavior; the G90D mutant formed an asymmetrical band with a maximal absorbance at 400 nm,

TABLE 1

Spectroscopic properties of WT and mutant rhodopsins

Rhodopsin	λ_{max} [a]	ϵ [b] $\times 10^3$	$A_{280}/A\lambda max$ [c]	Thermal bleaching $t_{1/2}$ [d]	NH$_2$OH reactivity $t_{1/2}$ [e]
	nm	*$M^{-1} cm^{-1}$*		*min*	*min*
WT-11*cis*	499 ± 1	42.7 ± 0.5	2.2 ± 0.1	133.4 ± 1.3	155.0 ± 10.0
G90V 11-*cis*-retinal	489 ± 1	36.0 ± 0.3	3.4 ± 0.2	3.8 ± 0.7	3.3 ± 0.7
G90D 11-*cis*-retinal	484 ± 2	37.1 ± 0.3	2.7 ± 0.1	114.2 ± 0.9	3.6 ± 1.1

[a] Mean value and S.D. of the visible peak of samples obtained in independent purifications ($n = 3$) of WT and mutant rhodopsin purified in Buffer C or D.

[b] Each ϵ value was calculated from the formula, $\epsilon = (A/A_{Rh})(A_{440Rh}/A_{440})\epsilon_{Rh}$, where A is the absorbance at the λ_{max} value, A_{440} is the absorbance at 440 nm after acid denaturation, and ϵ_{Rh} is the molar extinction of rhodopsin (42.7×10^3 M^{-1} cm^{-1}).

[c] The ratio of absorbance at 280 nm to λ_{max} provides an idea of both sample purity and the ability of opsin to form pigment with the chromophore. Data are mean $\pm$ S.D. values of independently purified proteins in Buffer C ($n = 3$).

[d] Thermal bleaching ($t_{1/2}$) of detergent-purified samples in Buffer D at 48 °C. Values are the mean $\pm$ S.D. ($n = 3$) of the time course decay of the visible peak absorbance (λ_{max}) normalized to that of WT rhodopsin. Data points were obtained by using the equation, $\Delta A = (A - A_f)/(A_0 - A_f)$, where A is the absorbance recorded at λ_{max}, A_f is the absorbance at the final time, and A_0 is the absorbance at time 0, and were fit to a single exponential decay function (G90V) or a linear function (WT and G90D).

[e] SB stability as determined by the rate constants of hydroxylamine reactivity of the dark state pigments at 20 °C. Values (mean $\pm$ S.D., $n = 3$) were determined by monitoring the rate of λ_{max} absorbance decrease after the addition of hydroxylamine (pH 7.0) to the samples in buffer D (final concentration of 50 mM) and adjusted to an exponential rise function with either a single component or a linear function.

whereas the G90V mutant showed a WT-like 440 nm protonated SB band. In the case of the G90D mutant, the band obtained upon acidification is probably due to contributions from both a 380 nm band corresponding to free retinal and to a protonated SB species at about 465 nm. This result suggests the presence of retinal already detached from the opsin moiety and agrees with previous studies (11).

MetaII Stability for G90V and G90D Rhodopsin Mutants— MetaII decay was determined, in real time, by monitoring Trp fluorescence increase upon rhodopsin illumination. $t_{1/2}$ values, derived from fluorescence curves (not shown) for G90V, reflected a slower decay (35 ± 2 min) when compared with WT (14 ± 2 min), but G90D showed a rapid decay process (<2 min).

Chemical and Thermal Stability of the Gly-90 Rhodopsin Mutants— Hydroxylamine reactivity was used as a measure of SB stability in the dark state for WT rhodopsin and the Gly-90 mutants (Fig. 3*A*). The SB in rhodopsin is remarkably stable in the presence of hydroxylamine in darkness but reacts rapidly upon illumination. Amino acid replacements that affect the SB environment have been shown to decrease the stability of mutant pigments in the presence of hydroxylamine (24). As expected, WT rhodopsin did not react with hydroxylamine under the conditions of the experiment, in the dark, during the time period analyzed. In contrast, each of the Gly-90 mutant pigments reacted with hydroxylamine in the dark, reflecting a less compact structure for the mutants in the SB linkage environment.

Another approach used to assess the G90V chromophore stability, in the dark state, was to follow the decay of the visible band at 55 °C. Due to the fast thermal decay for the G90V mutant at this temperature (data now shown), thermal stability was studied at 48 °C. At this latter temperature, the G90D mutant showed the same behavior as WT, and the G90V mutant showed a surprisingly faster thermal bleaching kinetics (Fig. 3*B*). In contrast, the chromophore regeneration rates were similar for the two Gly-90 mutants, both showing slower rates than WT rhodopsin (Fig. 3*C*).

Effect of 9-cis-Retinal on G90V Mutant Pigment Properties— The molecular properties of G90V mutant were also probed by regenerating the mutant receptor with the 9-*cis*-retinal analog. Although the regeneration mechanism is reported to be the same for both chromophores (9-*cis*-retinal and 11-*cis*-retinal) in the native receptor, interestingly, the G90V mutant rhodop-
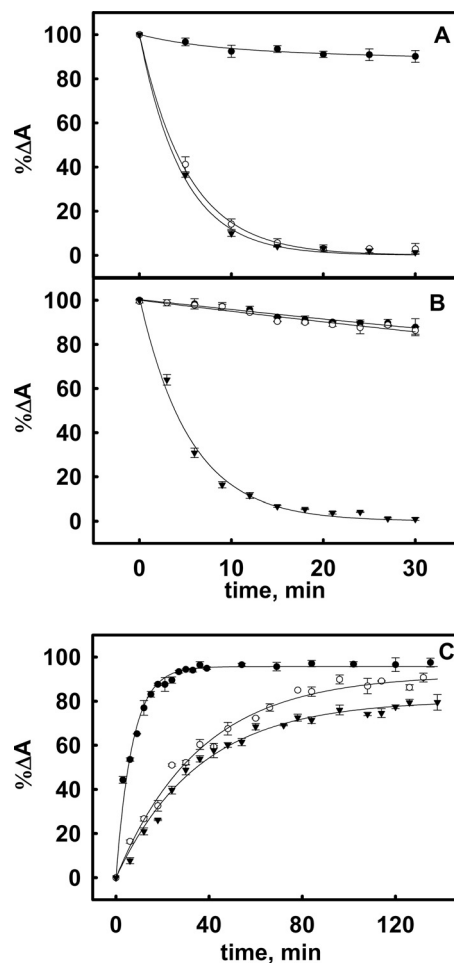

FIGURE 3. **Chemical and thermal stability and chromophore regeneration for WT and opsin mutant pigments.** *A*, hydroxylamine reactivity of SB linkage for the WT (●) and G90D (○) and G90V (▼) rhodopsin mutant pigments. Mutant rhodopsins, purified in Buffer D, were incubated with 50 mM hydroxylamine, pH 7.0, and the decrease of λ_{max} was recorded over time. *B*, thermal stability of WT (●), G90D (○), and G90V (▼) rhodopsins. Purified proteins were incubated at 48 °C in Buffer D, and the normalized absorbance values at the absorption maximum were plotted as a function of incubation time. The mutant data were fit with a single exponential function; WT data were fit with a linear function. *C*, chromophore regeneration rates for WT and Gly-90 mutant opsins purified in Buffer D. 11-*cis*-Retinal was added to samples, and regeneration rates were determined upon pigment illumination with light of $\lambda > 495$ nm. The G90V mutant showed slow retinal regeneration speed at 25 °C, which suggests a disturbance of the chromophore binding site by the Val side chain. These results are similar to those reported for the G90D mutant (51). *Error bars*, mean $\pm$ S.E.
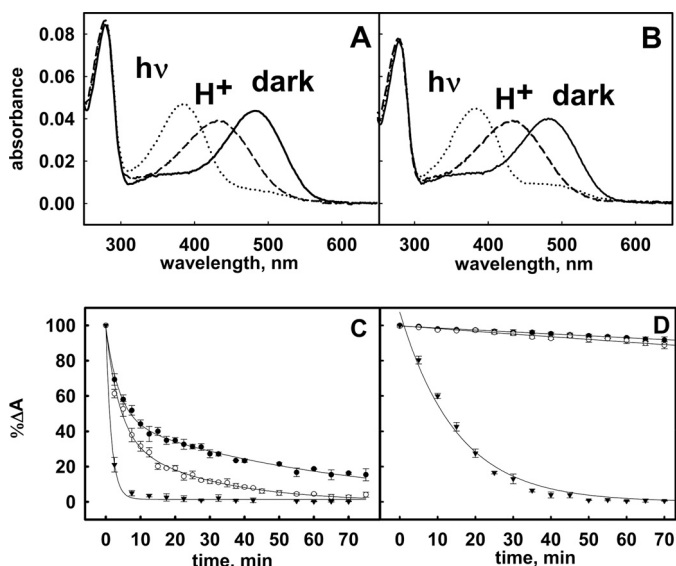
FIGURE 4. **Spectroscopic characterization of the G90V pigment regenerated with 9-*cis*-retinal compared with WT regenerated with 9-*cis*-retinal and 11-*cis*-retinal-regenerated G90V mutant.** The *upper panels* show UV-visible spectra of WT (*A*) and G90V (*B*) regenerated with 9-*cis*-retinal. Pigments were expressed in COS-1 cells and immunopurified with the Rho1D4 antibody in Buffer D. Dark spectra were recorded under dim red light conditions, illumination was performed at highest intensity of a $\lambda > 495$ nm light source for 10 s, and acidification was carried out by adding H_2SO_4. The *lower panels* show UV-visible data corresponding to the thermal (*C*) and hydroxylamine (*D*) assays for the 9-*cis*-retinal G90V pigment (○) compared with 9-*cis*-retinal WT (●) and 11-*cis*-retinal G90V mutant (▼). The 9-*cis*-retinal reconstituted G90V pigment showed increased chemical and thermal stability when compared with the 11-*cis*-retinal-regenerated mutant. Data were fit by a single exponential decay function ($y_0 + ae^{-bx}$). All data points are the mean average of three independent measurements ($n = 3$). *Error bars*, mean ± S.E.

sin showed better chromophore regeneration with 9-*cis*-retinal (Fig. 4*B* and Table 2) than with 11-*cis*-retinal (compare with Fig. 2*B* and Table 1). In this case, the A_{280}/A_{485} ratio of the purified 9-*cis*-retinal-regenerated G90V mutant was the same as WT rhodopsin regenerated with the same isomer (1.9) (Table 2). The photobleaching behavior was, however, similar to that observed for the 11-*cis*-retinal-regenerated sample with a remaining absorbance in the visible region after 10-s illumination. Thus, in the case of the G90V 9-*cis*-retinal rhodopsin, a fraction of the dark-visible absorbance species seems to be resistant to bleaching, after dim red light stimulation of the sample ($\lambda > 495$ nm), and slowly decays in the dark (data not shown). This could be attributed to the higher activation energy of 9-*cis*-retinal isomerization. The bend due to the *cis* double bond in the retinyl chain in 9-*cis*-retinal, located 2 positions before 11-*cis*-retinal, could provide an optimized fit into the binding pocket, and this might account for differences in stability between 9-*cis*-retinal- and 11-*cis*-retinal-regenerated pigments.

Further characterization of the G90V 9-*cis*-retinal rhodopsin showed a reversal of the instability seen for the 11-*cis*-retinal-regenerated sample. The hydroxylamine reactivity was dramatically reduced and recovered a WT-like behavior, and the thermal stability was also clearly improved, although it did not attain WT levels (Fig. 4, *C* and *D*; compare with Fig. 3, *B* and *A*, respectively). We also regenerated the G90D mutant with 9-*cis*-retinal for comparison with the 11-*cis*-retinal-regenerated mutant. In this case, we found that the chromophore regener-

ation was poor, and the thermal and chemical (hydroxylamine reactivity) stabilities were lower than those of G90V regenerated with the same retinal analog (data not shown). These results suggest that the binding pocket of G90V mutant can better accommodate the 9-*cis*-retinal isomer compared with the G90D mutant.

Transducin Activation by Purified Gly-90 Mutants—The ability of each of the Gly-90 mutants to catalyze guanine nucleotide exchange by transducin was assayed using a filter-binding assay method. In this assay, we could measure the activity in both opsin and rhodopsin states. Rhodopsin activity was measured in the dark and after photobleaching. We found a similar behavior for the mutants and the WT in the rhodopsin state in the dark and a similar rate for the mutants after illumination under our experimental conditions (Fig. 5). The main novel functional result here is that the G90V mutant shows constitutive activity in its opsin state (Fig. 5). We could also detect constitutive activity for G90D, which was consistent with previous reports (11).

DISCUSSION

Unraveling the molecular mechanisms underlying different phenotypes caused by rhodopsin mutations, like CSNB and RP, is important to develop targeted therapies. The G90V rhodopsin mutation, in TM2 of rhodopsin, was reported to cause RP (16). Another mutation at the same position, G90D, has been thoroughly studied as a mutation causing CSNB (11, 25–27), a milder clinical phenotype with rod cell dysfunction but little rod or cone cell degeneration, if any, and a better prognosis than RP. Thus, the G90D and G90V mutations affect the same amino acid of the protein, yet they result in distinct clinical phenotypes. We decided to compare the molecular features of the two mutants, side by side, in an effort to further clarify the mechanisms of retinal degeneration and dysfunction in RP and the CSNB milder condition at a molecular level.

The UV-visible spectral properties of the G90V mutant, in the dark, were similar to those of the G90D mutant and showed a blue-shifted visible absorbance band as a result of the introduced perturbation at the SB linkage region, in the vicinity of the Glu-113 counterion. The A_{280}/A_{489} ratio was only slightly increased in the case of the G90V mutant, suggesting no critical folding defect for this mutant receptor. Subcellular localization experiments showed that the mutant is correctly trafficked to the PM, and its pattern did not vary significantly from that of WT rhodopsin. This, again, argues against a folding problem as the main cause of the mutant behavior, contrary to what has been proposed for Class II mutants like P23H (18, 28) or the modeling proposed for G90V (16). In contrast, G90V photobleaching behavior is altered, with formation of a distinguishable photointermediate upon illumination. This altered photointermediate formation has been proposed to affect the metarhodopsin conformation equilibria and to be one of the potential molecular defects associated with some RP mutants (29).

An unexpected relevant finding is that the thermal stability of the chromophore, in the dark, for G90V is dramatically decreased when compared with the G90D mutant and WT protein, which show similar stability (Fig. 3*B*). The formation and

TABLE 2

Spectroscopic properties of WT and G90V rhodopsin regenerated with 9-*cis*-retinal

Rhodopsin	$\lambda_{max}{}^a$	$\epsilon^b \times 10^3$	$A_{280}/A\lambda max^c$	Thermal bleaching $t_{1/2}{}^d$	NH_2OH reactivity $t_{1/2}{}^e$
	nm	$M^{-1} cm^{-1}$		*min*	*min*
WT 9-*cis*-retinal	486 ± 3	43.2 ± 0.1	1.9 ± 0.1	9.7 ± 1.3	435.0 ± 15.0
G90V-9-*cis*-retinal	480 ± 2	34.1 ± 0.5	1.9 ± 0.1	4.4 ± 0.5	327.0 ± 8.0

[a] Mean value and S.D. of the visible peak of samples obtained in independent purifications ($n = 3$) in Buffer D.

[b] Each ϵ value was calculated from the formula, $\epsilon = (A/A_{Rh})(A_{440Rh}/A440)\epsilon_{Rh}$, where A is the absorbance at the λ_{max} value, A_{440} is the absorbance at 440 nm after acid denaturation, and ϵ_{Rh} is the molar extinction of rhodopsin ($42.7 \times 10^3\ M^{-1}\ cm^{-1}$).

[c] The ratio of absorbance at 280 nm to λ_{max} provides an idea of both sample purity and the ability of opsin to form pigment with the chromophore. Data are the mean $\pm$ S.D. values of independently purified proteins ($n = 3$).

[d] Thermal bleaching ($t_{1/2}$) of purified samples in Buffer D at 48 °C. Values are the mean $\pm$ S.D. ($n = 3$) of the time course decay of the visible peak absorbance (λ_{max}) normalized to that of WT rhodopsin. Data points were obtained by using the equation, $\Delta A = (A - A_f)/(A_0 - A_f)$, where A is the absorbance recorded at λ_{max}, A_f is the absorbance at the final time, and A_0 is the absorbance at time 0, and were fit to a single exponential decay function.

[e] Schiff base stability as determined by the rate constants of hydroxylamine reactivity of the dark state pigments at 20 °C. Values (mean $\pm$ S.D., $n = 3$) were determined by monitoring the rate of λ_{max} absorbance decrease after the addition of 50 mM hydroxylamine (pH 7.0) to the samples in buffer D and adjusted to a single exponential decay function (G90D and G90V) or a linear function (WT).
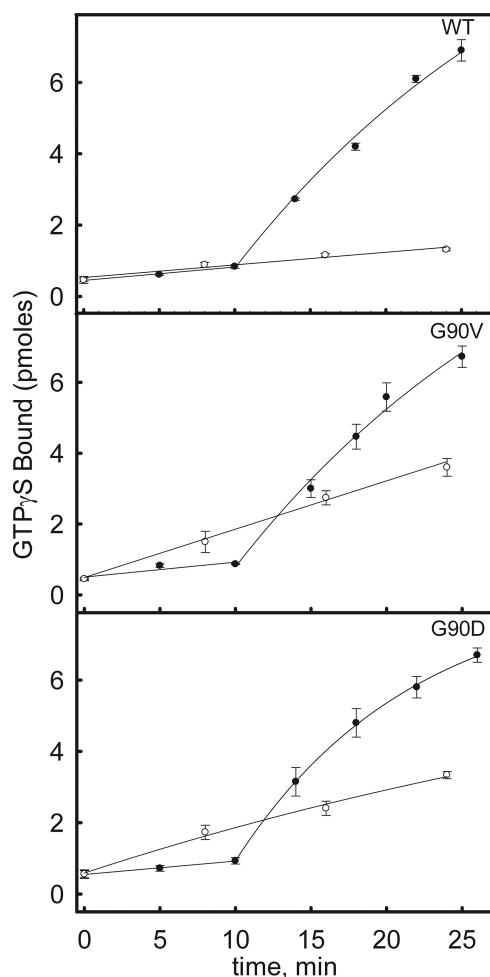

FIGURE 5. **Transducin activation by WT and Gly-90 mutant opsins.** In order to test the G90V mutant for potential constitutive activity, the activity of each Gly-90 mutant and WT, in the opsin and rhodopsin states, was measured by means of a radioactive filter-binding assay in COS cell membranes. G90D and G90V mutants and WT opsin (○) and rhodopsin (●) activity were measured by means of a radionucleotide filter-binding assay in COS cell membranes obtained in Buffer A. The assay was performed in the dark by mixing opsin or rhodopsin and transducin in 25 mM Tris, pH 7.5, 100 mM NaCl, 5 mM magnesium acetate, 5% glycerol, 2.5 mM DTT, and 3 μM [35S]GTPγS. Reactions were initiated by the addition of opsin or rhodopsin, and samples were filtrated at different times in the dark and after illumination (at minute 10). The mean and S.E. (*error bars*) of three independent measurements are represented.

accumulation of abnormal photointermediates and the low thermal stability of the chromophore have also been recently pointed out as triggering factors of retinal degeneration associated with rhodopsin adRP (6). The decreased chemical stability of G90V, in the presence of hydroxylamine in the dark, suggests that this mutation disturbs the SB environment, in agreement with the reported properties of G90D (26). The altered counterion-chromophore interaction could presumably render the SB more accessible to the solvent and to hydroxylamine in the dark. Therefore, given the fact that Gly-90 mutant opsins are able to bind 11-*cis*-retinal and to form functional pigments either in detergent solution or in COS-cell membranes, we conclude that the instability of the G90V mutant pigment purified in detergent is a result of greater susceptibility of the SB linkage to hydrolysis.

Previous studies on rhodopsin mutants (18, 30–34) led to the conclusion that the mutant opsins were misfolded based on low pigment yield, intracellular accumulation, altered glycosylation, or non-native disulfide bonds but did not provide direct evidence for defects in protein thermal stability or folding kinetics (35). However, several mutant rhodopsins associated with adRP were shown to exhibit decreased thermal stability (36–38), which suggests that thermal instability may be a common property of a given subset of adRP mutant opsins, and it may be possible to correlate the degree of instability with progress of the disease and to develop therapeutic approaches using retinoids or other agents as pharmacological chaperones.

The reported effects of Gly-90 mutants suggest an important role of a functional water molecule present in the vicinity of Glu-113 and the SB in the dark state crystal structure of rhodopsin. This water molecule binds to both the carbonyl backbone and one of the carboxyl oxygen atoms of Glu-113, and its free energy of binding has been estimated to be −10 kcal/mol.[4] The fact that such energy is among the largest values in rhodopsin indicates that this is a functional or structurally important water molecule. The model in Fig. 6 shows how the lack of side chain at Gly-90 provides an empty volume that is filled with such a water molecule, whereas the hydrophobic chain in G90V either would not allow the water molecule to be accommodated or would result in a lower affinity. In WT rhodopsin, this water molecule seems to be involved in the deprotonation step of SB in MetaII, by lowering the pK_a of Glu-113 (39–41). The lack of the water molecule would alter the metarhodopsin I to MetaII transition energy landscape and would also decrease dark state

---

[4] R. Osman, A. Cordomi, T. Lazaridis, M. Mezei, and L. Pardo, manuscript in preparation.
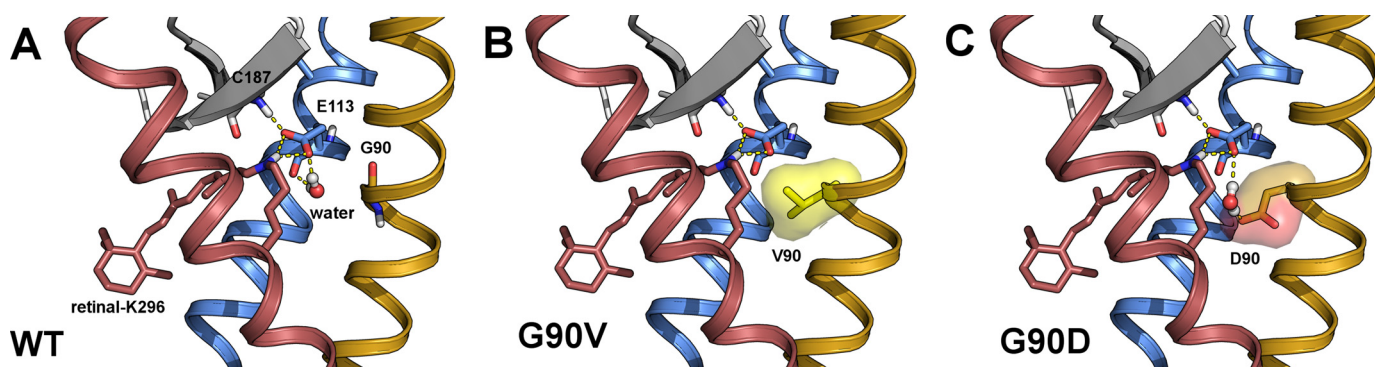
FIGURE 6. **Schematic model of the environment of the SB and Glu-113 in the WT and in Gly-90 mutants.** TM2 (*gold*), TM3 (*blue*), and TM7 (*pale red*) are shown with a schematic diagram. The remaining helices have been omitted for clarity. Important residues are shown as *sticks*, and the water molecule bound to Glu-113 is represented with *balls* and *sticks*. *Dashed lines* indicate hydrogen bond interactions. Val-90 and Asp-90 are highlighted with a *surface*. Shown are the rhodopsin 1GZM structure (*A*), G90V (*B*), and G90D (*C*) models after energy minimization using Amber99SB force field (52). Images were created using PyMol (53).

stability, in agreement with the present results. In the case of G90D, it is likely that the water molecule can still be accommodated with a small rearrangement of neighboring residues. Previous spectroscopic measurements suggested that the G90D mutant would have some of the features of the activated rhodopsin, including a protonated Glu-113 (24). In that case, the protonation of Glu-113 would lower the strength of the hydrogen bonds with the SB and with the backbone of Cys-187 in the second extracellular loop. This is in agreement with the high hydroxylamine reactivity observed for this mutant.

TMs in rhodopsin are not regular α-helices (42). In the case of TM2, the abnormal configuration is associated with the presence of the adjacent Gly residues (Gly-89 and Gly-90). The Gly-Gly pattern is a conserved sequence in visual pigments (43). The Gly side chain can adopt conformational angles that other amino acids cannot adopt. Helix bend and the consequential structural twist derived are thought to be key structural features to the conformational changes occurring in G-protein-coupled receptor activation, stressing the functional significance of this sequence pattern in the rhodopsin receptor (44). The Val substitution results in more bulkiness near the protein backbone, restricting the conformations that the main chain can adopt (45), and this could affect accommodation of the structural water molecule described above.

Our results suggest that G90D and G90V mutants cannot be referred to as misfolding mutations because they are able to bind 11-*cis*-retinal, and they traffic through the secretory pathway to the PM in cell culture. Furthermore, they show a similar capacity to activate the G-protein transducin as the WT under light conditions. The G90D mutant has been shown to activate transducin constitutively, and it was proposed previously that this constitutive activity was due to the G90D opsin (*i.e.* the mutated opsin without the bound chromophore) (46). However, a recent *in vivo* study, using photoreceptor cells from G90D transgenic mice, proposed that dark activity, and not constitutive activity, would be the cause of cell desensitization (47). Interestingly, we find here that the G90V mutant associated with adRP can activate transducin constitutively, a behavior that was only seen for another adRP mutant, K296E. This mutant was proposed to cause RP due to its ability to sequester

cellular components needed for the shut-off process, such as arrestin, rather than its constitutive activity (48). Thus, our results indicate that constitutive activity may be associated with RP for certain rhodopsin mutants (maybe those in the close proximity of the SB linkage), but structural instability seems to be required to trigger the RP phenotype.

The G90V substitution has some of the properties of a class IV mutant (mutants that "do not necessarily affect folding but affect rod-opsin stability and posttranslational modification") (9). We have no evidence of altered posttranslational modifications with G90V, but of the six classes previously proposed, it resembles a class IV mutation (9). In any case, taking into account that we find constitutive activity for G90V in the opsin state, this mutant also shows some features of class VI mutations (9). The clinical phenotype of the visual disorders associated with both mutations, CSNB with G90D and RP with G90V, must be a consequence of differences in the dark-inactive structural conformation of the mutant receptor, which is thermally unstable in the case of the G90V mutation. This lower stability, alone or in combination with the formation of altered activation photointermediates upon illumination (29), could affect the rhodopsin cycle of intermediates, altering the normal rhodopsin turnover and prompting receptor malfunction and accumulation, which could trigger photoreceptor cell death associated with RP.

In addition to its native chromophore, 11-*cis*-retinal, opsin can also accommodate 9-*cis*-retinal without suffering any major structural changes in the TM region and keeping the same orientation of the amino acid side chains in the retinal binding pocket (49). We find an increased stability of the 9-*cis*-retinal rhodopsin G90V mutant compared with the 11-*cis*-retinal-regenerated mutant, which is in agreement with previous reports suggesting a role for retinoids as pharmacological chaperones (6). According to previous studies, an alternative pathway could occur in the eye enabling a visual response in RPE65 knock-out mice by alternative using minute amounts of 9-*cis*-retinal present in their retinas (50). Whether the effect seen for G90V regenerated with 9-*cis*-retinal can play a role in the retinal degeneration process associated with G90V rhodopsin is to be further explored.

REFERENCES

1. Palczewski, K. (2006) *Annu. Rev. Biochem.* **75,** 743–767
2. Matsuyama, T., Yamashita, T., Imai, H., and Shichida, Y. (2010) *J. Biol. Chem.* **285,** 8114–8121
3. Manyosa, J., Andres, A., Buzon, V., and Garriga, P. (2003) *Med. Clin. (Barc.)* **121,** 153–157
4. Gregersen, N., Bross, P., Vang, S., and Christensen, J. H. (2006) *Annu. Rev. Genomics Hum. Genet.* **7,** 103–124
5. Carrell, R. W. (2005) *Trends Cell Biol.* **15,** 574–580
6. Krebs, M. P., Holden, D. C., Joshi, P., Clark, C. L., 3rd, Lee, A. H., and Kaushal, S. (2010) *J. Mol. Biol.* **395,** 1063–1078
7. Surguchev, A., and Surguchov, A. (2010) *Brain Res. Bull.* **81,** 12–24
8. Green, E. S., Menz, M. D., LaVail, M. M., and Flannery, J. G. (2000) *Invest. Ophthalmol. Vis. Sci.* **41,** 1546–1553
9. Mendes, H. F., van der Spuy, J., Chapple, J. P., and Cheetham, M. E. (2005) *Trends Mol. Med.* **11,** 177–185
10. Dryja, T. P., Berson, E. L., Rao, V. R., and Oprian, D. D. (1993) *Nat. Genet.* **4,** 280–283
11. Rao, V. R., Cohen, G. B., and Oprian, D. D. (1994) *Nature* **367,** 639–642
12. Gross, A. K., Rao, V. R., and Oprian, D. D. (2003) *Biochemistry* **42,** 2009–2015
13. Zeitz, C., Gross, A. K., Leifert, D., Kloeckener-Gruissem, B., McAlear, S. D., Lemke, J., Neidhardt, J., and Berger, W. (2008) *Invest. Ophthalmol. Vis. Sci.* **49,** 4105–4114
14. McAlear, S. D., Kraft, T. W., and Gross, A. K. (2010) *Adv. Exp. Med. Biol.* **664,** 263–272
15. Zhukovsky, E. A., and Oprian, D. D. (1989) *Science* **246,** 928–930
16. Neidhardt, J., Barthelmes, D., Farahmand, F., Fleischhauer, J. C., and Berger, W. (2006) *Invest. Ophthalmol. Vis. Sci.* **47,** 1630–1635
17. Oprian, D. D., Molday, R. S., Kaufman, R. J., and Khorana, H. G. (1987) *Proc. Natl. Acad. Sci. U.S.A.* **84,** 8874–8878
18. Saliba, R. S., Munro, P. M., Luthert, P. J., and Cheetham, M. E. (2002) *J. Cell Sci.* **115,** 2907–2918
19. Liu, X., Garriga, P., and Khorana, H. G. (1996) *Proc. Natl. Acad. Sci. U.S.A.* **93,** 4554–4559
20. Mendes, H. F., and Cheetham, M. E. (2008) *Hum. Mol. Genet.* **17,** 3043–3054
21. Sakmar, T. P., Franke, R. R., and Khorana, H. G. (1989) *Proc. Natl. Acad. Sci. U.S.A.* **86,** 8309–8313
22. Farrens, D. L., and Khorana, H. G. (1995) *J. Biol. Chem.* **270,** 5073–5076
23. Kosmaoglou, M., Kanuga, N., Aguilà, M., Garriga, P., and Cheetham, M. E. (2009) *J. Cell Sci.* **122,** 4465–4472
24. Ramon, E., del Valle, L. J., and Garriga, P. (2003) *J. Biol. Chem.* **278,** 6427–6432
25. Sieving, P. A., Richards, J. E., Naarendorp, F., Bingham, E. L., Scott, K., and Alpern, M. (1995) *Proc. Natl. Acad. Sci. U.S.A.* **92,** 880–884
26. Zvyaga, T. A., Fahmy, K., Siebert, F., and Sakmar, T. P. (1996) *Biochemistry* **35,** 7536–7545
27. Woodruff, M. L., Olshevskaya, E. V., Savchenko, A. B., Peshenko, I. V., Barrett, R., Bush, R. A., Sieving, P. A., Fain, G. L., and Dizhoor, A. M. (2007) *J. Neurosci.* **27,** 8805–8815
28. Illing, M. E., Rajan, R. S., Bence, N. F., and Kopito, R. R. (2002) *J. Biol. Chem.* **277,** 34150–34160
29. Bosch-Presegué, L., Ramon, E., Toledo, D., Cordomí, A., and Garriga, P. (2011) *FEBS J.* **278,** 1493–1505
30. Doi, T., Molday, R. S., and Khorana, H. G. (1990) *Proc. Natl. Acad. Sci. U.S.A.* **87,** 4991–4995
31. Sung, C. H., Davenport, C. M., Hennessey, J. C., Maumenee, I. H., Jacobson, S. G., Heckenlively, J. R., Nowakowski, R., Fishman, G., Gouras, P., and Nathans, J. (1991) *Proc. Natl. Acad. Sci. U.S.A.* **88,** 6481–6485
32. Sung, C. H., Schneider, B. G., Agarwal, N., Papermaster, D. S., and Nathans, J. (1991) *Proc. Natl. Acad. Sci. U.S.A.* **88,** 8840–8844
33. Kaushal, S., and Khorana, H. G. (1994) *Biochemistry* **33,** 6121–6128
34. Hwa, J., Klein-Seetharaman, J., and Khorana, H. G. (2001) *Proc. Natl. Acad. Sci. U.S.A.* **98,** 4872–4876
35. Noorwez, S. M., Malhotra, R., McDowell, J. H., Smith, K. A., Krebs, M. P., and Kaushal, S. (2004) *J. Biol. Chem.* **279,** 16278–16284
36. Noorwez, S. M., Kuksa, V., Imanishi, Y., Zhu, L., Filipek, S., Palczewski, K., and Kaushal, S. (2003) *J. Biol. Chem.* **278,** 14442–14450
37. Janz, J. M., Fay, J. F., and Farrens, D. L. (2003) *J. Biol. Chem.* **278,** 16982–16991
38. Andrés, A., Garriga, P., and Manyosa, J. (2003) *Biochem. Biophys. Res. Commun.* **303,** 294–301
39. Yan, E. C., Kazmi, M. A., Ganim, Z., Hou, J. M., Pan, D., Chang, B. S., Sakmar, T. P., and Mathies, R. A. (2003) *Proc. Natl. Acad. Sci. U.S.A.* **100,** 9262–9267
40. Vogel, R., Siebert, F., Yan, E. C., Sakmar, T. P., Hirshfeld, A., and Sheves, M. (2006) *J. Am. Chem. Soc.* **128,** 10503–10512
41. Mahalingam, M., Martínez-Mayorga, K., Brown, M. F., and Vogel, R. (2008) *Proc. Natl. Acad. Sci. U.S.A.* **105,** 17795–17800
42. Deupi, X., Dölker, N., López-Rodríguez, M. L., Campillo, M., Ballesteros, J. A., Pardo, L. (2007) *Curr. Top. Med. Chem.* **7,** 991–998
43. Horn, F., Vriend, G., and Cohen, F. E. (2001) *Nucleic Acids Res.* **29,** 346–349
44. Benned-Jensen, T., and Rosenkilde, M. M. (2009) *Curr. Mol. Pharmacol.* **2,** 140–148
45. Filipek, S., Teller, D. C., Palczewski, K., and Stenkamp, R. (2003) *Annu. Rev. Biophys. Biomol. Struct.* **32,** 375–397
46. Li, T., Franson, W. K., Gordon, J. W., Berson, E. L., and Dryja, T. P. (1995) *Proc. Natl. Acad. Sci. U.S.A.* **92,** 3551–3555
47. Dizhoor, A. M., Woodruff, M. L., Olshevskaya, E. V., Cilluffo, M. C., Cornwall, M. C., Sieving, P. A., and Fain, G. L. (2008) *J. Neurosci.* **28,** 11662–11672
48. Jin, S., Cornwall, M. C., and Oprian, D. D. (2003) *Nat. Neurosci.* **6,** 731–735
49. Sekharan, S., Sugihara, M., Weingart, O., Okada, T., and Buss, V. (2007) *J. Am. Chem. Soc.* **129,** 1052–1054
50. Fan, J., Rohrer, B., Moiseyev, G., Ma, J. X., and Crouch, R. K. (2003) *Proc. Natl. Acad. Sci. U.S.A.* **100,** 13662–13667
51. Gross, A. K., Xie, G., and Oprian, D. D. (2003) *Biochemistry* **42,** 2002–2008
52. Hornak, V., Abel, R., Okur, A., Strockbine, B., Roitberg, A., and Simmerling, C. (2006) *Proteins* **65,** 712–725
53. DeLano, D. L. (2010) *The PyMOL Molecular Graphics System*, version 1.2r3pre, Schrödinger, LLC, New York